Bull. Mater. Sci., Vol. 35, No. 5, October 2012, pp. 823–832. © Indian Academy of Sciences.

Effect of sintering temperature and heating mode on consolidation of Al–7Zn–2·5Mg–1Cu aluminum alloy

C PADMAVATHI*, A UPADHYAYA and D AGRAWAL†

Department of Materials Science and Engineering, Indian Institute of Technology, Kanpur 208 016, India
†Materials Research Institute, Pennsylvania State University, University Park, USA

MS received 19 April 2011; revised 4 January 2012

Abstract. Densification behaviour, phase transformation, microstructural evolution and hardness values of microwave sintered Al–7Zn–2·5Mg–1Cu (7775) aluminum alloy were investigated and compared with conventionally sintered samples. Microwave sintering was performed in 2·45 GHz multimode microwave furnace at temperatures ranging from 570–630 °C. Microwave sintering at a heating rate of as high as 22°C/min resulted in ∼55% reduction of processing time as compared to conventional sintering. A lower sintered density observed in the case of microwave processed samples was attributed to the inhomogeneity in microstructure and phase distribution. The X-ray diffraction results of conventionally sintered samples showed the presence of $MgZn_2$, Mg_2Zn_{11} and $CuMgAl_2$, while only $MgZn_2$ and $CuMgAl_2$ phases were found in the case of microwave sintered samples and in lesser amount. Higher hardness and high standard deviation values were noticed for microwave sintered samples as compared to conventional counterparts.

Keywords. Aluminum alloys; microwave sintering; densification.

1. Introduction

The sintered Al–Zn–Mg–Cu alloys are gaining importance in automotive industries (Danninger *et al* 1998) due to their lightweight and higher strength combined with advantages offered by powder metallurgical (P/M) processing (Hunt 1998). Prealloyed or master-alloy powders mixed with elemental powders are pressed and sintered to obtain higher densification with improved dimensional stability (German 1994; German *et al* 2009). Successful sintering of aluminum alloys was found to occur in the presence of liquid phase thereby amount of the liquid phase determines the densification and mechanical properties (Schaffer 2001; Schaffer *et al* 2001a). Liquid phase sintering mechanism of aluminum alloys involves the following steps: liquid formation, particle re-arrangement, solution re-precipitation, grain shape accommodation, pore-filling and finally solid state sintering (German 1985; Sercombe 1998). Extensive research work has been done on the effect of chemical composition (Gradl *et al* 2004) sintering parameters (time, temperature, atmosphere and heating rate) (Schaffer and Huo 1999; Schaffer 2000; Martin *et al* 2002; Martin and Castro 2003; Shahmohammadi *et al* 2007) particle size (Lumley and Schaffer 1996) and addition of trace elements (Schaffer *et al* 2001b) on sintering response of Al–Zn–Mg–Cu alloy. The formation of transient or persistent liquid phase and heating rate employed during sintering influences dimensional stability, microstructure and mechanical properties of high strength Al–Zn–Mg–Cu alloy (Martin and Castro 2003). Microwave sintering provides rapid and volumetric heating (Roy *et al* 1999). In the last decade there have been many reports on application of microwave energy for sintering of metallic powders like ferrous (iron, steel and stainless steel) and non-ferrous (tungsten heavy alloys, bronze, molybdenum, etc) (Agrawal 2000; Anklekar *et al* 2001; Sethi *et al* 2003; Panda *et al* 2006, 2007; Padmavathi *et al* 2007; Upadhyaya and Sethi 2007; Upadhyaya *et al* 2007; Chhillar *et al* 2008; Mondal *et al* 2010). The literature available on MW sintering of aluminum alloys is negligible as compared to conventional sintering. For the first time Leparoux *et al* (2002) reported successful MW sintering of Al–SiC. Gupta and his co-workers (2005, 2007) demonstrated MW sintering of various Al-based composites. Microwave heating of metallic powders (Al–Cu–Fe) to single phase was first reported by Vauchera *et al* (2008). To the best of our knowledge, microwave sintering of 7xxx series alloys (Al–Zn–Mg–Cu) has so far not been critically evaluated. The present study investigates densification behaviour, phase transformation, microstructure development, conductivity and hardness values of Al–Zn–Mg–Cu alloy powders consolidated using 2·45 GHz microwave furnace and conventional furnace. The effect of heating mode and sintering temperature are discussed in detail in terms of above mentioned attributes.

2. Experimental

The as-received Al–7Zn–2·5Mg–1Cu (7775) powders containing 1·5 wt % acrawax were supplied by AMPAL Inc.,

*Author for correspondence (padmavathi.chandran@gmail.com)

USA. The composition and physical properties of powders are given in table 1. The morphology of alloy powder was studied using scanning electron microscopy (SEM) and irregular shaped particles were observed in figure 1. The 7775 powders were pressed in the range of 100–500 MPa into cylindrical pellets of 16 mm diameter and 6 mm height using uniaxial semi-automatic hydraulic press. Prior to sintering, compacts were delubricated for 6 h at 350 °C in a conventional vacuum furnace (10^{-2} torr). The transverse rupture strength (TRS) samples (31·7 × 12·7 × 5 mm) were prepared according to MPIF specification 41 and in the case of tensile testing, flat dog-bone shaped specimens were prepared as per MPIF specification 10.

Conventional sintering characteristics were investigated initially under vacuum (10^{-6} torr) in a SiC tubular furnace (supplier: Mahendra Instruments, India) at a constant heating rate of 5°C/min under 570–630 °C for 1 h. For comparison purpose, conventional sintering was also done under high purity N_2 in a SiC heated tubular furnace (supplier: Bysakh & Co, Kolkata, India). Microwave sintering was carried out in a 2·45 GHz, multimode microwave furnace (Cober Electronics, USA) with a variable output power of 6 kW under N_2. The delubricated samples were placed in a mullite based package made from fiberfrax. To ensure better microwave coupling, the package microwave transparent insulation also consisted of graphite coated SiC rods. Temperature measurements were done using infrared pyrometer (Raytek, Marathon series). The IR pyrometer was coupled with software for data acquisition based on emissivity of 0·4, as emissivity varied with temperature. The densities of the samples were determined using dimensional measurements as well as by Archimedes principle. The densification parameter was calculated to normalize sintered density which is described elsewhere (German 1994).

Microstructural examination of polished sintered alloys was conducted using an optical microscopy (Zeiss, Germany) and SEM (model: QUANTA 200, FEI, The Netherlands) along with EDS analysis. X-ray powder diffractometer (Rich Seifert & Co., Germany) based on Cu-Kα radiation (with $\lambda = 0{\cdot}154$ nm) with a scan rate of 3 deg/min was carried out to analyse the phases. XPS analysis was done using monochromatic Al Kα source instruments (Kratos, Axis Ultra, UK) operating at 14 kV and 20 mA. All spectra were referenced to C 1*s* peak with a binding energy of 285 eV. Electrical conductivity was measured using digital conductivity meter (model: 757, Technofour, India). Mechanical properties such as microhardness, transverse rupture strength and tensile properties were measured for sintered compacts. Vicker's microhardness measurements were done using Vicker's hardness tester (Model: SHP 150, Barieiss, Germany) with a load of 20 g for 10 s. The tensile testing was conducted on 7775 sintered bars using a universal testing machine (model: 1195, INSTRON, UK) at a crosshead speed of 0·5 mm/min and SEM of fractured surfaces was studied.

Table 1. Chemical composition and physical characteristics of as-received 7775 alloy powders.

Properties of 7775 alloy powder	
Composition (wt.%)	Al–7Zn–2·5Mg–1·0Cu
Processing route	Gas atomization
Particle size, μm	
D_{10}	27
D_{50}	88
D_{90}	181
Apparent density, g/cm^3	1·36
Flow rate, s/50 g	18·70
Specific surface area, m^2/g	0·135
Theoretical density, g/cm^3	2·81

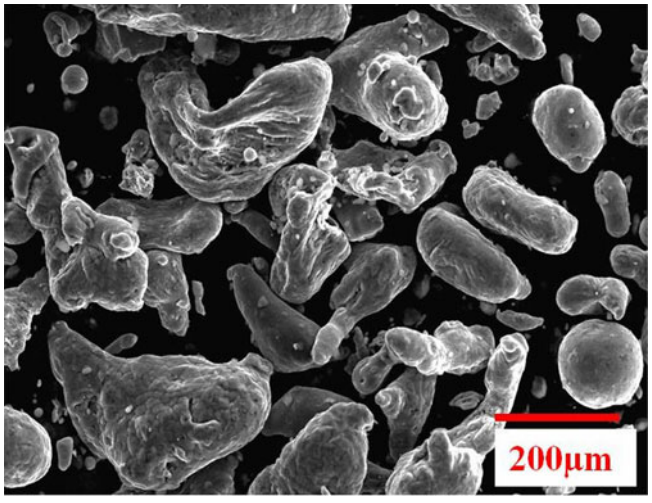

Figure 1. Scanning electron microscopy of 7775 aluminum alloy powder.

3. Results and discussion

3.1 *Green compact characteristics*

Figures 2a and b show scanning electron microstructure along with its respective EDS spectrum of 7775 alloy compact mainly comprising of Al peak and minor peaks corresponding to Zn, Mg and Cu. Figure 2 also reveals the whitish regions at the interparticle boundaries in two distinct microstructures viz. elongated (Zn-rich) and spherical (Mg-rich) implying that Mg and Zn are present in admixed condition. The compaction characteristics for the 7775 alloy powder presented in table 2 shows that highest green density (~93·8%TD) was obtained for a compaction pressure of 400 MPa or higher. To evaluate the effect of porosity on densification, compacts pressed at 200 and 400 MPa were used for sintering.

3.2 *Thermal profile of 7775 alloy in different heating modes*

Figure 3 compares thermal profile for 7775 aluminum alloy compacts consolidated through the conventional and

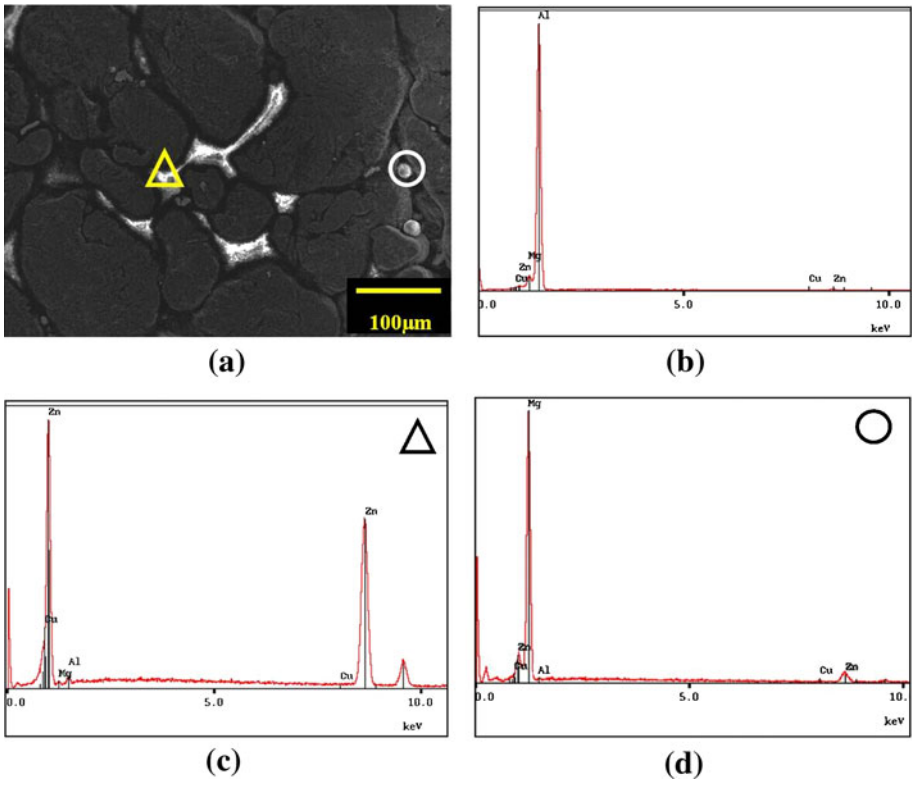

Figure 2. (**a**) SEM, (**b**) EDS area analysis, (**c**) and (**d**) EDS spot analysis of as-pressed 7775 compact.

Table 2. Effect of compaction pressure on green density of 7775 compacts.

Compaction pressure (MPa)	Green density, % theoretical
100	89 ± 0·5
200	91 ± 0·8
300	93 ± 0·2
400	94 ± 0·5
500	94 ± 0·5

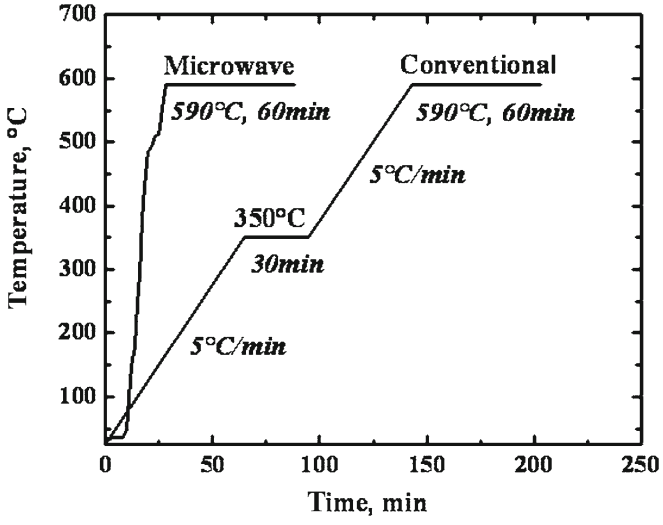

Figure 3. Comparison of thermal profiles of 7775 compact heated in conventional and microwave furnace.

microwave furnace. It is quite interesting to note that the 7775 Al alloy powder compact coupled well with microwaves and got heated up rapidly. The overall compact heating rate obtained in the microwave furnace is 22 °C/min, whereas in conventional furnace it is restricted to 5 °C/min. The rapid heating using microwaves resulted in about 55% reduction in the processing time as compared to longer processing time and isothermal holds at intermediate temperatures in the case of conventional sintering. Microwave heating in metals is quite different from that observed in ceramic materials (Roy *et al* 1999). The depth of penetration in metals also known as skin-depth (δ) defined as the distance into the material at which the incident powers drop to $1/e$ (36·8%) of the surface value. The skin depth is mathematically expressed as follows (Mishra *et al* 2006):

$$\delta = \frac{1}{\sqrt{\pi f \mu \sigma}} = 0{\cdot}029\sqrt{\rho \lambda_0}, \tag{1}$$

Table 3. Effect of compaction pressure and sintering temperature on densification of 7775 alloy sintered in conventional vacuum furnace.

Sintering temperature (°C)	Sintered density (% Th)		Densification parameter	
Compaction pressure (MPa)	200	400	200	400
570	84	85	−0·8	−1·4
590	84	86	−0·7	−1·2
610	86	87	−0·6	−1·1
630	87	92	−0·4	−0·3

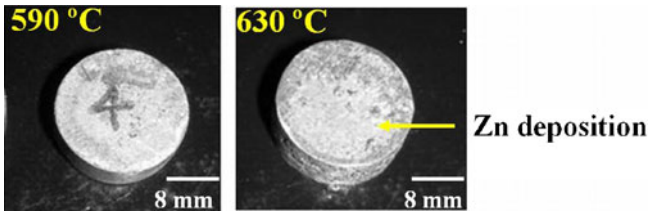

Figure 4. Photographs of 7775 alloy sintered under vacuum at 590 °C and 630 °C in conventional furnace.

where f is the microwave frequency (2·45 GHz), μ the magnetic permeability, σ the electrical conductivity, ρ the electrical resistivity, λ_0 the incident wavelength (12·24 cm for 2·45 GHz waves). The skin depth of aluminum was calculated using the above expression and found to be very low at ∼1·7 μm (Padmavathi 2010). With the increasing temperature and resistivity, the skin depth also increases (Mishra *et al* 2006; Padmavathi 2010). In this respect, the microwave sintering of aluminum is very difficult.

3.3 *Densification response of 7775 alloy*

Table 3 compares effect of compaction pressure and sintering temperature on densification of 7775 alloy heated in conventional vacuum furnace. Highest sintered density (91·6%) and densification parameter (−0·3) were exhibited by compacts pressed at 400 MPa and sintered at 630 °C due to the extensive liquid formation via super solidus liquid phase sintering (SLPS). All the 7775 compacts show swelling behaviour. In the case of vacuum sintering, oxide removal by Mg was more effective in order to obtain strong Al–Al bonds; however, the Zn loss via vapour (Lumley and Schaffer 1999) could be detrimental to the properties of alloy. Figure 4 shows photographs of 7775 alloy sintered in conventional furnace at 590 °C and 630 °C; it is observed that there was no distortion in any of the sintered compacts. The closer examination of surface reveals the whitish regions on top and side surface of the compacts. This is attributed to the Zn evaporated from the compact during heating cycle and deposited on the surface during cooling cycle. Hence it is not advisable to sinter Al–Zn–Mg–Cu alloys in vacuum furnace. Therefore, nitrogen atmosphere was considered for further investigation.

Figure 5 summarizes effect of heating mode and sintering temperature on densification response of 7775 alloy under N_2. With exception of few compacts, sintering under both heating modes shows an improvement in sintered density with increase in sintering temperature and compaction pressure. The microwave sintered compacts show inferior densification response as compared to conventionally sintered compacts. Overall, the extent of swelling reduces with increase in sintering temperature from 570–630 °C at a given compaction pressure in both heating modes. This suggests that there are competing processes, viz. transient liquid phase sintering (TLPS) which causes swelling and solid-state and/or SLPS that contributes to densification (Shahmohammadi *et al* 2008) at higher temperatures (630 °C). It is worth noticing that the densification results are similar to those reported by Schaffer *et al* (2001b) of premixed Al–8Zn–2·5Mg–1Cu and sintered beyond 610 °C; while other reports (Savitskii and Martsunova 1977; Martin and Castro 2003; Shahmohammadi *et al* 2007; Kim *et al* 2004) suggest that sintering at 610 °C results in higher density. This difference in densification response may be possibly due to the difference in Zn content in the alloy composition and amount of the liquid formed. Also in case of composites (Roy *et al* 2008) lesser density obtained of nano-TiO_2 dispersed $Al_{65}Cu_{20}Ti_{15}$ microwave sintered samples is attributed to poorer coupling of microwave energy with Al matrix at 500 °C. The 7775 alloys sintered at 630 °C showed better sintered density due to increased penetration depth with increasing temperature; aiding in absorption of microwave energy by Al alloy (Mishra *et al* 2006) as compared to their (Roy *et al* 2008) work. Similarly, microwave sintering of titanium powders also resulted in lower or somewhat comparable sintered densities to that of conventional route (Luo *et al* 2010).

3.4 *Effect of heating mode on microstructure and phase evolution*

Figures 6 and 7 compare effect of heating mode and sintering temperature on the microstructures of 7775 alloy. In the case of conventional sintering, compacts sintered at 630 °C exhibit more well-defined and equiaxed grains, revealing the grain boundaries which are intact than 590 °C. This is due

to the extensive liquid phase formation via SLPS and higher diffusion rates yielding densification (German 1985) without any shape distortion. The microstructure of microwave sintered compacts reveals a differential contrast along grain boundaries at both sintering temperatures. This may be due to the fact that shorter processing times in MW sintering leads to non-uniform diffusion of alloying species and accumulation of the same along the grain boundaries (figure 6b).

Figures 7a and b show corresponding SEM microstructures of 7775 alloy consolidated in both heating modes. SEM of conventionally sintered compact at 630 °C shows precipitation of some phases from interior of solid solution grain into grain boundaries leaving pinhole pores in grains called precipitation-induced densification (Lumley and Schaffer 1999). For microwave compacts sintered at 630 °C, large accumulation of liquid phase were noticed at grain boundaries with tiny pores near grain periphery arranged like pearls in a necklace. Moreover, microwave sintered compacts at both temperatures resulted in more amount of liquid phase along the grain boundaries as compared to conventional ones. As a result of higher heating rate, the transient liquid and atoms/elements present at intermediate temperature do not get sufficient time to diffuse into the Al matrix. Consequently, microstructure of microwave sintered compacts

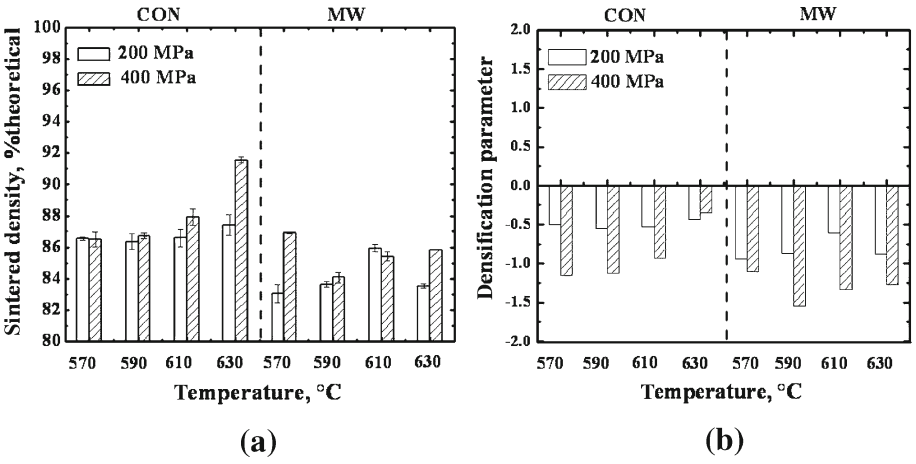

Figure 5. Effect of sintering temperature and heating mode of 7775 alloy under N_2 on (**a**) sintered density and (**b**) densification parameter.

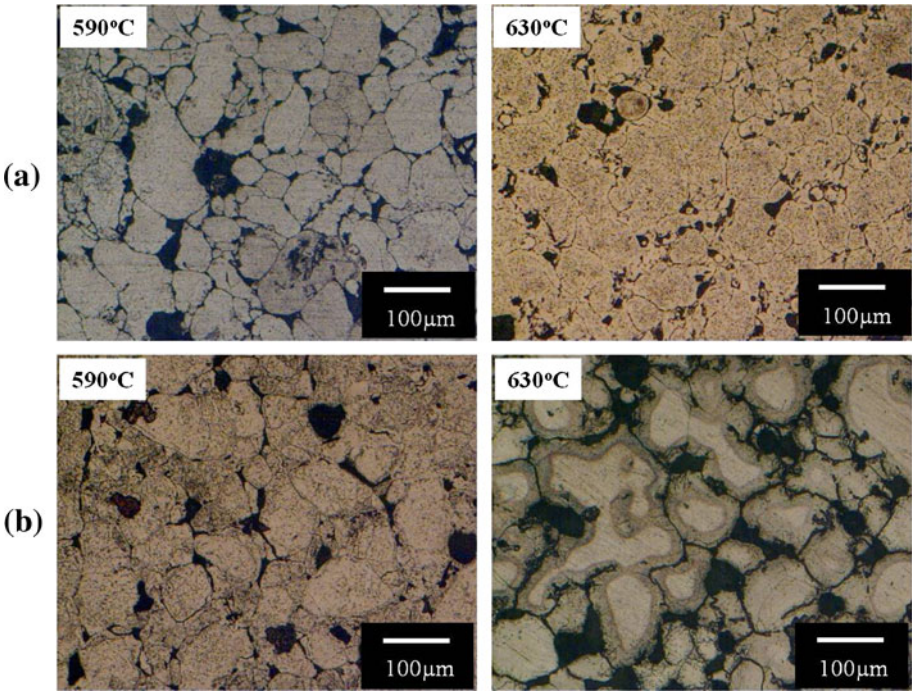

Figure 6. Optical microstructures of 7775 alloy pressed at 400 MPa sintered in nitrogen at 590 °C and 630 °C consolidated through (**a**) conventional and (**b**) microwave furnace.

is very inhomogeneous and coarser pores. Microstructural inhomogenization of microwave sintered premixed Cu–Sn alloys was reported by Upadhyaya and Sethi (2007). At temperatures exceeding 590 °C, the SLPS plays an important role in densification of both microwave and conventionally sintered compacts.

Figures 8a and b compare XRD patterns of compacts sintered in conventional and microwave furnace at different temperatures. For both the heating modes, α-Al is a major phase that forms. Besides α-Al (JCPDS file number: 85-1327), conventionally sintered samples contain $MgZn_2$ (JCPDS file number: 77-1177), $CuMgAl_2$ (JCPDS file number: 28-0014) and Mg_2Zn_{11} (JCPDS file number: 06-0664) phases, whereas microwave sintered compacts show only $CuMgAl_2$ and $MgZn_2$ phases. Mg and Zn are expected to react and form Mg_2Zn_{11} and other similar intermetallics with varying stoichiometries (e.g. $MgZn_2$) at intermediate temperatures depending upon heating modes. The peak intensities of α-Al and $CuMgAl_2$ decrease as the sintering temperature increases from 570–630 °C. Lower amount of intermetallic phases at all sintering temperatures is noticed for the microwave sintered compacts. XRD studies also confirm that the presence of intermetallics $MgZn_2$, Mg_2Zn_{11} and $CuMgAl_2$ are the main cause of liquid phase formation depending upon heating modes.

Figure 9 shows XPS analysis of as-pressed and microwave sintered compacts at 630 °C. The microwave sintered compacts contain higher amounts of Zn (i.e. high intensity Zn

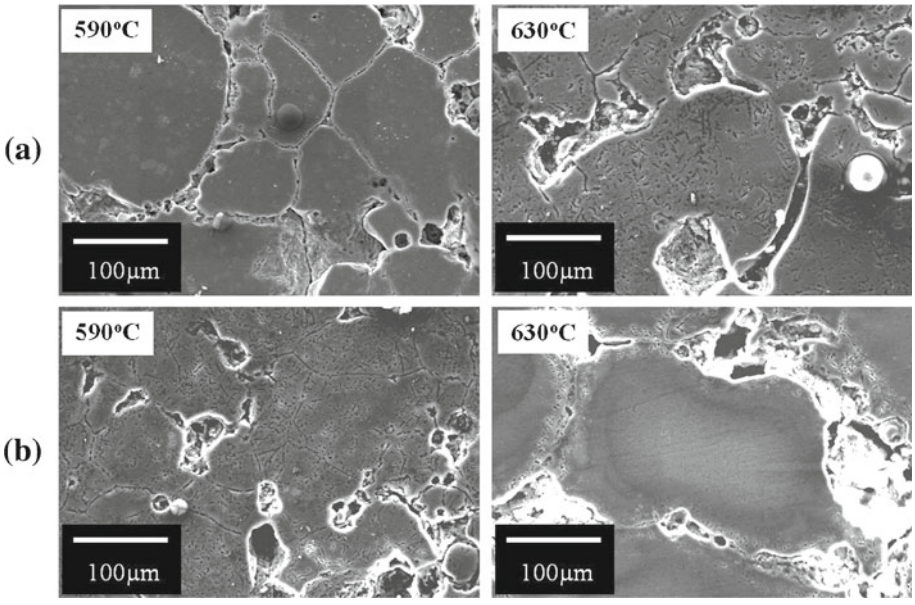

Figure 7. SEM of 7775 alloy pressed at 400 MPa sintered in nitrogen at 590°C and 630 °C consolidated through (**a**) conventional and (**b**) microwave furnace.

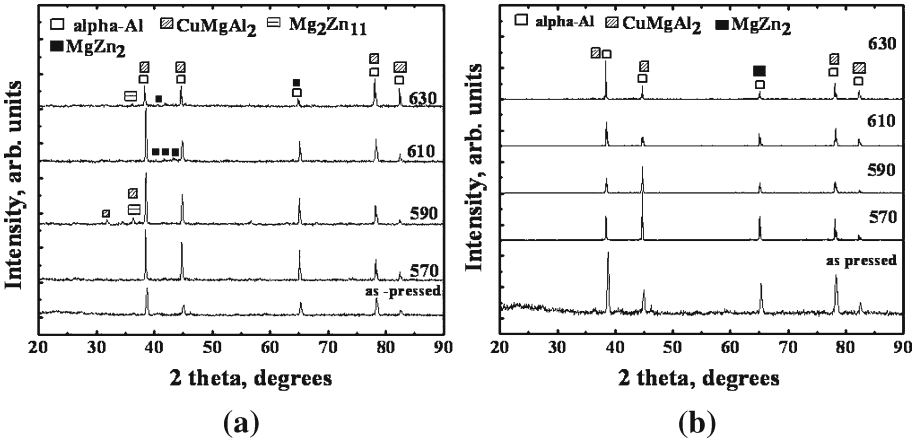

Figure 8. XRD analysis of 7775 alloy sintered at different temperatures in (**a**) conventional and (**b**) microwave furnace.

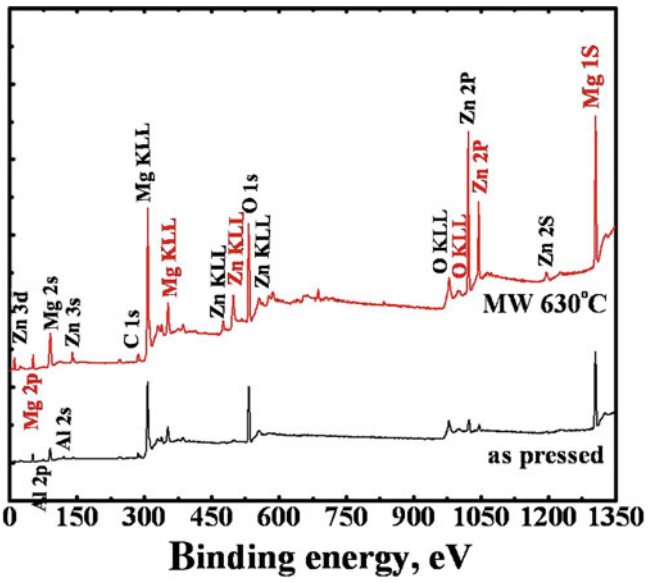

Figure 9. XPS analysis of as-pressed and microwave sintered compacts at 630 °C under N_2.

peaks) on surface of broken samples which confirmed that eutectic melt was not completely diffused. The presence of Mg and O in higher amounts support the formation of spinel structure which facilitates densification by breaking oxide layer. Figure 10 shows photoelectron/auger lines corresponding to (a) Mg 1*s*, (b) O 1*s*, (c) Al/Mg/Zn and (d) Zn 2*p* peaks of 7775 alloy sintered in N_2. The Mg 1*s* peak with binding energy of 1305·18 eV can be related to spinel ($MgAl_2O_4$) formation. The enrichment of Mg, O_2 at surface of sintered compacts indicate that nitrogen atmosphere can reduce the oxygen content in presence of Mg. The presence of Al/Mg/Zn peaks may indicate the formation of eutectic liquids in sintered compacts.

3.5 *Effect of heating mode on properties evolution of 7775 alloy*

Figures 11a and b summarize effect of heating mode and sintering temperature on conductivity and hardness. Irrespective of heating modes, increase in temperature results in improvement of electrical conductivity and hardness. The efficacy of microwave sintering on both these properties has

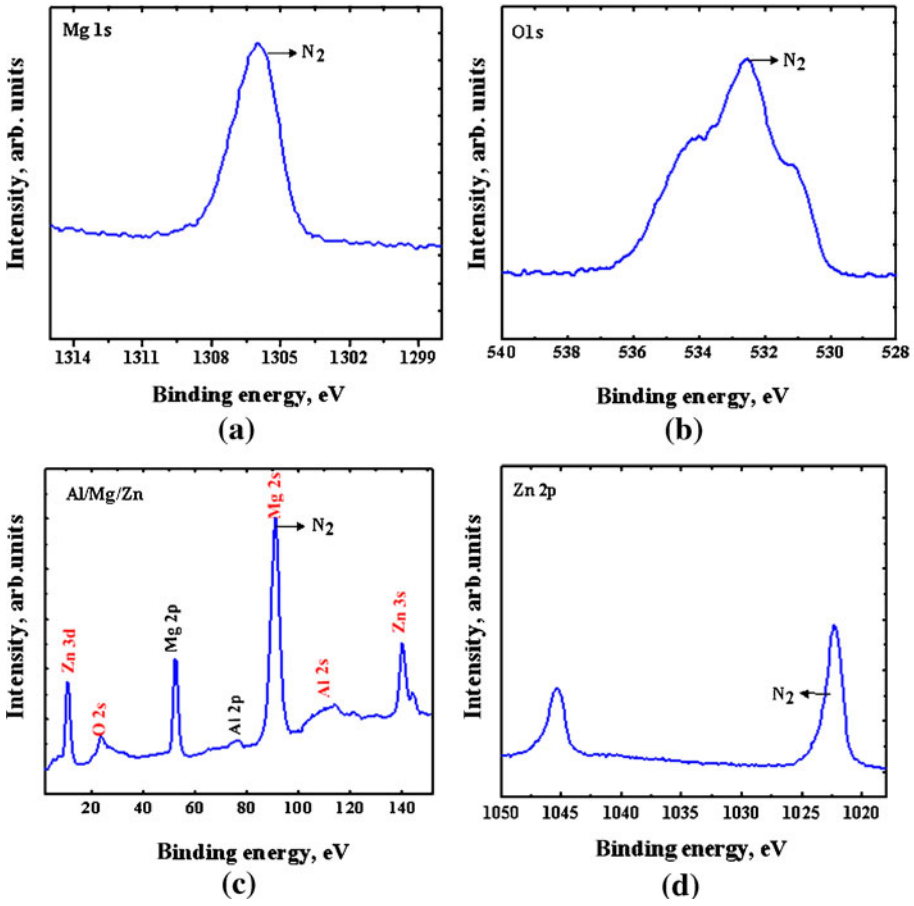

Figure 10. Photoelectron/auger lines corresponding to (**a**) Mg 1*s*, (**b**) O 1*s*, (**c**) Al/Mg/Zn and Zn 2*p* peaks of 7775 alloy sintered at 630 °C in nitrogen atmosphere.

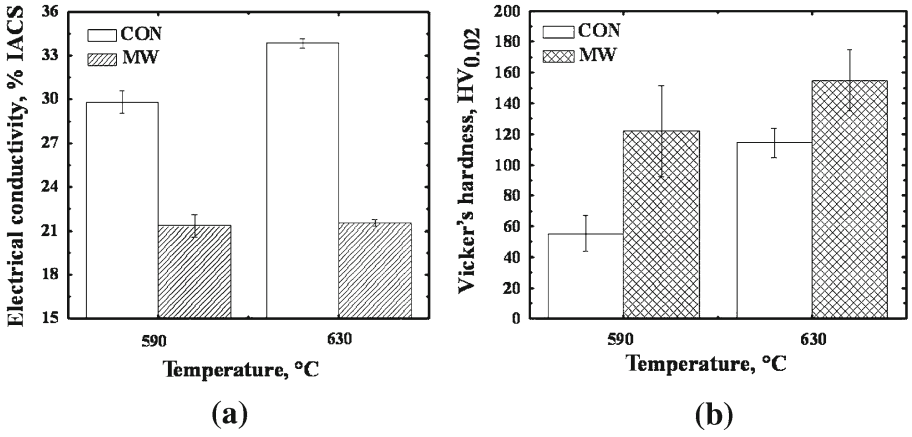

Figure 11. Effect of sintering temperature and heating mode of 7775 alloy sintered under N_2 on (**a**) electrical conductivity and (**b**) hardness.

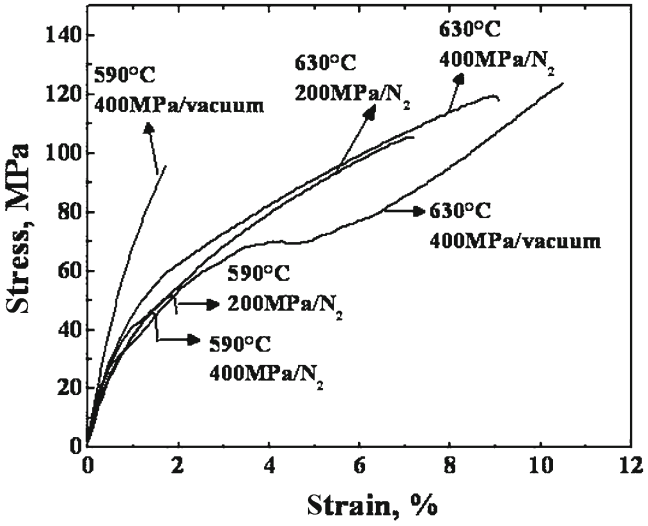

Figure 12. Tensile stress–strain curves of 7775 alloy pressed at 200 and 400 MPa, sintered in nitrogen and vacuum at 590 °C and 630 °C.

an opposing trend. As compared to conventional sintering, the conductivity drastically decreases by about 40% in alloys consolidated through microwaves at both temperatures. The reason for this behaviour may be attributed to the microstructural inhomogeneity and poor densification. Microwave sintered compacts at both sintering temperatures showed higher hardness and standard deviation values.

Higher hardness in the case of MW sintering was due to the presence of melt pools at the grain boundaries. These melt pools consist of majority of the alloying elements and left undiffused owing to shorter cycle times. However, presence of porosity and non-uniform distribution of these liquid pools would have resulted in high standard deviation in the hardness values as compared to conventionally sintered counterparts. Due to distortion and cracking, tensile and compression properties of microwave sintered compacts could not be extensively characterized and therefore, are not discussed.

Figure 12 compares tensile stress–strain curves of 7775 alloy processed using variable pressure and sintering temperature. The strength and ductility values are summarized in table 4. Overall the 7775 alloy compacts pressed at 400 MPa and sintered at 630 °C exhibit the highest strength (TRS:147 MPa, UTS:119 MPa, YS: 101 MPa) and ductility (6·4%). It shows that vacuum sintered compacts also resulted in higher TRS, UTS and ductility values at 630 °C. This type of behaviour may be attributed to the fine-grained, SLPS microstructure and presence of intermetallics

Table 4. Effect of compaction pressure and sintering temperature on transverse rupture strength and tensile properties sintered in conventional furnace under vacuum and N_2.

Sintering temperature/ atmosphere, °C	Compaction pressure, MPa	Transverse rupture strength, MPa	Yield strength MPa	Ultimate tensile strength (MPa)	Elongation, %
590/N_2	200	125 ± 1·3	33 ± 1·2	52 ± 0·9	0·3 ± 2·6
	400	132 ± 1·8	27 ± 2·0	46 ± 1·9	0·7 ± 1·1
630/N_2	200	125 ± 0·5	92 ± 0·8	110 ± 0·7	6·2 ± 0·5
	400	147 ± 0·6	101 ± 0·8	119 ± 0·6	6·4 ± 0·3
590/vacuum	400	241 ± 1·1	64 ± 2·1	96 ± 1·9	2·4 ± 2·1
630/vacuum	400	244 ± 0·4	101 ± 0·2	124 ± 0·4	7·1 ± 0·6

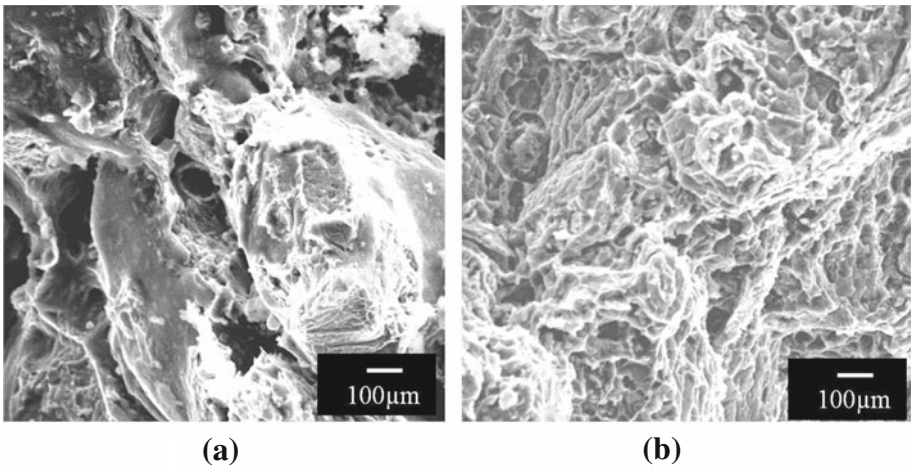

Figure 13. SEM fractographs of 7775 alloy sintered at 630 °C under (**a**) vacuum and (**b**) nitrogen.

at the grain boundaries. Precipitation induced densification mechanism also makes the grains softer by oozing out alloying elements leading to higher ductility. Fractography of vacuum and nitrogen sintered compacts at 630 °C show dimples on the fractured surface as an indication of ductile mode of failure as shown in figure 13.

4. Conclusions

In summary, this study compares densification response of Al–7Zn–2·5Mg–1Cu (7775) alloy consolidated in conventional and microwave furnaces as a function of sintering temperature. The microwave sintering resulted in about 55% reduction in processing time as compared to conventional sintering. Microwave sintered alloy showed poor sinterability due to the microstructural inhomogeneity and coarser pores as compared with conventionally sintered compacts. The microstructural inhomogeneity is most likely caused as a result of high heating rate, the transient liquid and intermetallics that form do not get sufficient time to diffuse into the Al matrix. Higher sintering temperature (630 °C) resulted in equiaxed grains and liquid phase formation occurred via SLPS with higher diffusion rates yielding densification in conventional mode. The hardness and its standard deviation values of microwave sintered samples were found to be higher due to the presence of melt pool and non-uniform distribution of these liquid pools at the grain boundaries.

Acknowledgements

The authors would like to thank Mr Jessu Joys of AMPAL Inc., Palmerton, USA, for providing the 7775 aluminum alloy powders for the present study. This study was conducted under the Networked Centre for Microwave Processing of Metal-Ceramic Composites funded by the Indo-US Science and Technology Forum (IUSSTF), New Delhi, India.

References

Anklekar R M, Agrawal D K and Roy R 2001 *Powder Metall.* **44** 355

Agrawal D 2000 *Proc. PM World Cong.* (Kyoto, Japan: JPMA) p. 797

Chhillar P, Agrawal D and Adair J H 2008 *Powder Metall.* **51** 182

Danninger H, Neubing H C and Gradl J 1998 *Proc. PM World Cong. Granada Spain EPMA* **5** 272

German R M 1994 *Powder metallurgy science* (New Jersey: MPIF) 2nd ed.

German R M 1985 *Liquid phase sintering* (New York: Plenum Press) 1st ed. p. 1

German R M, Suri P and Park S J 2009 *J. Mater. Sci.* **44** 1

Gradl J, Neubing H C and Muller A 2004 *Proc. PM world cong.* (Vienna: EPMA) p. 13

Gupta M and Wong W L E 2005 *Scr. Mater.* **52** 479

Gupta M and Wong W L E 2007 *Microwaves and metals* (Singapore: John Wiley & Sons Ltd) 1st ed., p. 190

Hunt W H Jr 1998 *Proc. PM, Al and light alloys for automotive applications* (New Jersey, Princeton: MPIF) **1** p. 1

Kim Y D, Min K H, Kang S P and Chang S Y 2004 *Proc. PM world cong.* (Vienna: EPMA) p. 39

Lumley R N and Schaffer G B 1996 *Scr. Mater.* **35** 589

Lumley R N and Schaffer G B 1999 *Metall. Mater. Trans.* **A30** 1682

Luo S, Bettles C J, Yan M, Schaffer G B and Qian Ma 2010 *Key Engg. Mater.* **436** 141

Leparoux S, Vaucher S and Beffort O 2002 *Werkstofftechnol. Kollo.* **24–25** 13

Martin J M, Gomez-Acebo T and Castro F 2002 *Powder Metall.* **45** 173

Martin J M and Castro F 2003 *J. Mater. Process. Technol.* **143–144** 814

Mishra P, Sethi G and Upadhyaya A 2006 *Metall. Mater. Trans.* **B37** 839

Mondal A, Upadhyaya A and Agrawal D 2010 *Int. J. Refract. Metals Hard Mater.* **28** 597

Panda S S, Singh V, Upadhyaya A and Agrawal D 2006 *Metall. Mater. Trans.* **A37** 2253

Panda S S, Upadhyaya A and Agrawal D 2007 *J. Mater. Sci.* **42** 966

Padmavathi C, Upadhyaya A and Agrawal D 2007 *Scr. Mater.* **57** 651

Padmavathi C 2010 *Liquid phase sintering of 2712, 6711 and 7775 aluminum alloys and their properties*, Ph.D. Thesis, Indian Institute of Technology, Kanpur

Roy D, Chakravarthy D, Mitra R and Manna I 2008 *J. Alloys Compd* **460** 320

Roy R, Agrawal D K, Cheng J and Gedevanishvili S 1999 *Nature* **399** 668

Savitskii A P and Martsunova L S 1977 *Sovt. Powder Metall. Metal Ceram.* **5** 14

Schaffer G B and Huo S H 1999 *Powder Metall.* **42** 219

Schaffer G B 2000 *Powder Metall.* **43** 163

Schaffer G B 2001 *Mater. Technol. Adv. Perf. Mater.* **16** 237

Schaffer G B, Sercombe T B and Lumley R N 2001a *Mater. Chem. Phys.* **67** 85

Schaffer G B, Huo S H, Drennan J and Auchterlonie G J 2001b *Acta Mater.* **49** 2671

Sercombe T B 1998 *Non-conventional sintered aluminum powder alloys*, Ph.D. Thesis, The Queensland University, Australia

Sethi G, Upadhyaya A, Agrawal D K and Roy R 2003 *Sci. Sinter.* **35** 49

Shahmohammadi M, Simchi A, Danninger H and Arvand A 2007 *Mater. Sci. Forum* **534–536** 489

Shahmohammadi M, Simchi A and Gierl C 2008 *Powder Metall.* **8** 1

Upadhyaya A and Sethi G 2007 *Scr. Mater.* **56** 469

Upadhyaya A, Tiwari S K and Mishra P 2007 *Scr. Mater.* **56** 5

Vauchera S S, Nicula R, Civera J M C, Schmitt B and Patterson B 2008 *J. Mater. Res.* **23** 170